Dear Author,

Please, note that changes made to the HTML content will be added to the article before publication, but are not reflected in this PDF.

Note also that this file should not be used for submitting corrections.

Science of the Total Environment xxx (2015) xxx–xxx

Contents lists available at ScienceDirect

Science of the Total Environment

journal homepage: www.elsevier.com/locate/scitotenv

A model-based analysis of SO_2 and NO_2 dynamics from coal-fired power plants under representative synoptic circulation types over the Iberian Peninsula

Víctor Valverde [a,*], María T. Pay [a], José M. Baldasano [a,b]

[a] Earth Sciences Department, Barcelona Supercomputing Center-Centro Nacional de Supercomputación, Barcelona, Spain
[b] Environmental Modeling Laboratory, Technical University of Catalonia, Barcelona, Spain

HIGHLIGHTS

- Synoptic circulation controls coal-fired power plants plumes from Atlantic facilities.
- A combination of synoptic and mesoscale circulations drives Mediterranean plumes.
- Under Atlantic dominated circulation types, pollution plumes can reach up to 250 km.
- Emission injection within the PBL favours fumigation close to the source (<20 km).
- Hourly contribution to SO_2 and NO_2 ranges 2–25 μg m^{-3} and 1–15 μg m^{-3}, respectively.

GRAPHICAL ABSTRACT

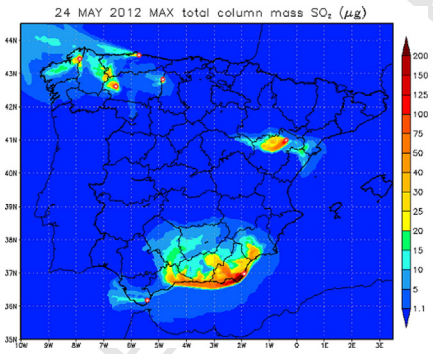

ARTICLE INFO

Article history:
Received 13 May 2015
Received in revised form 21 September 2015
Accepted 22 September 2015
Available online xxxx

Warning: Editor name is missing. Please check.

Keywords:
Synoptic classification
Coal-fired power plants
SO_2/NO_2 plumes dynamics
CALIOPE-AQFS
Air quality modelling

ABSTRACT

Emissions of SO_2 and NO_2 from coal-fired power plants are a significant source of air pollution. In order to typify the power plants' plumes dynamics and quantify their contribution to air quality, a comprehensive characterisation of seven coal-fired power plant plumes has been performed under six representative circulation types (CTs) identified by means of a synoptic classification over the Iberian Peninsula. The emission and the transport of SO_2 and NO_2 have been simulated with the CALIOPE air quality forecasting system that couples the HERMES emission model for Spain and WRF and CMAQ models. For the facilities located in continental and Atlantic areas (As Pontes, Aboño, and Compostilla) the synoptic advection controls pollutant transport, however for power plants located along the Mediterranean or over complex-terrains (Guardo, Andorra, Carboneras, and Los Barrios), plume dynamics are driven by a combination of synoptic and mesoscale mountain–valley and sea–land breezes. The contribution of power plants to surface concentration occurs mainly close to the source (<20 km) related to a fumigation process when the emission injection takes place within the planetary boundary layer reaching up to 55 μg SO_2 m^{-3} and 32 μg NO_2 m^{-3}. However, the SO_2 and NO_2 plumes can reach long distances (>250 km from the sources) especially for CTs characterised by Atlantic advection.

* Corresponding author at: Earth Science Department, Barcelona Supercomputing Center-Centro Nacional de Supercomputación (BSC-CNS), Jordi Girona 29, Edificio Nexus II, 08034 Barcelona, Spain.
E-mail addresses: victor.valverde@bsc.es (V. Valverde), maria.pay@bsc.es (M.T. Pay), jose.baldasano@bsc.es (J.M. Baldasano).

http://dx.doi.org/10.1016/j.scitotenv.2015.09.111
0048-9697/

55 Mesoscale
56 Emissions

1. Introduction

Air pollution is a threat for human health (Brunekreef and Holgate, 2002; Gurjar et al., 2010; WHO, 2013) and the environment (de Vries et al., 2014). In the last years, the European Union has established limits to the emission of air pollutants (National Emission Ceilings Directive 2001/81/EC) and legally binding limit values for air quality (Directive 2008/50/EC) in order to reduce the exposition of people and ecosystems to harmful concentrations of pollutants. Partially due to these policy actions, during the 2001–2012 period, the SO_2 and NO_2 concentration at the remote rural European Monitoring and Evaluation Programme (EMEP) stations in Spain declined 3.6 to 7.7%/year and 2.8 to 3.7%/year, respectively (Querol et al., 2014)..

Despite the increase in renewable electricity production in Spain by 50% in the 2008–2012 period (REE, 2013) and the use of cleaner technologies and fuels (ORDEN PRE/77/2008), the contribution of coal-fired power plants to the electricity generation pool was 19.3% in 2012, 54,721 GWh for the Spanish Iberian Peninsula (REE, 2013), being the second technology in electricity generation in 2012 after nuclear (22.1%) and before wind power (18.1%). Although SO_2 and NO_2 emissions from energy industry (SNAP01) have been reduced by 29.7% and 12.5% during the period 2008–2012, respectively (MAGRAMA, 2014); they were still significant in 2012 corresponding to a 41% and 22% of the SO_2 and NO_2 total Spanish emissions, respectively. The emissions from coal-fired power plants were the main contributor within the SNAP01 with 79% and 55% of SO_2 and NO_2 emissions, respectively.

The synoptic scale circulation is considered to play a significant role in air pollution both transporting primary and secondary pollutants through long distances (Vivanco et al., 2012; Putero et al., 2014) and controlling the effect on the local meteorological conditions (Kassomenos et al., 1998; Menut et al., 1999, Segura et al., 2013). Several studies relate how different circulation types (CTs) establish dissimilar effects on health for respiratory (Jamason et al., 1997; de Pablo et al., 2013), cardiovascular, and digestive diseases (Morabito et al., 2006, de Pablo et al., 2008).

Circulation-type classification summarises a complex series of synoptic conditions into a catalogue containing a small number of predominant modes of atmospheric circulation or CTs (Barry and Perry, 1974; Beck and Philipp, 2010; Philipp et al., 2014). Each CT is associated with a number of distinctive meteorological behaviours and predominant flow characteristics (Shahgedanova et al., 1998). Several CT classifications have been performed over the Iberian Peninsula (IP) for different applications. Recently, an objective classification based on a climatic database has been developed for air quality purposes and could be used to analyse the plume dynamics under representative CTs (Valverde et al., 2014).

The dispersion of the pollutants emitted at high stacks relies on combination of meteorological fields and is affected by topography (Palau et al., 2005, 2009). Plume dispersion at power plants, refineries and incinerators has been analysed in impact assessments studies under particular pollution episodes over Spain (Salvador et al., 1992; Hernández et al., 1995, 1997; Puig et al., 2008; Baldasano et al., 2014). However, there is no a comprehensive characterisation of the plume dynamics from coal-fired power plants considering the influence of (1) the facilities characteristics, (2) the topography, and (3) the synoptic conditions affecting the IP. Understanding the plume dynamics and the specific contribution of power plants to air pollution under representative CTs can improve the power grid management in the context of environmental sustainability.

The objective of this work is twofold. First, to characterise the plume dynamics for selected Spanish coal-fired power plants under representative CTs over the IP, describing the role of emissions, meteorology, and topography. Second, to determine the contribution of SO_2 and NO_2 surface concentration of each power plant under each CT.

The paper is organised as follows. Section 2 describes the methods and data used. Section 3 characterises the power plants' plume dynamics and analyses their contribution to surface SO_2 and NO_2 concentration. Finally, Section 4 discusses the synoptic circulation role on plume dynamics over the IP.

2. Methods

This section presents the facilities that have been chosen for this study together with the circulation type classification used. The CALIOPE air quality forecasting system (CALIOPE-AQFS), whose characteristics are presented, is used in a case study context to characterise the power plants plume's dynamics.

2.1. Power plants selection

There are currently sixteen Spanish coal-fired power plants (combustion installations with boilers >300 MWt) in the IP. Seven facilities have been selected for this study considering those with highest contribution in terms of energy generation (>950 GWh $year^{-1}$) (Table 1 and Fig. 1). They represent 63.7% of the installed capacity and 79.4% of the 2009 electricity production of coal-fired power plants.

2.2. Selection of the episodes of study

The present work uses the synoptic classification established in Valverde et al. (2014) which objectively identifies six CTs over the IP (Table 2 and Fig. 2) over the present climate (1983–2012). The three most common CTs account for 67.6% of climatic frequency and mainly occur in the summertime, replacing one another. NWadv (23.9%) is a N/NW advective pattern characterised by the arrival of polar maritime air masses towards the IP; IBtl (22.4%) depicts a reduced pressure surface gradient, enabling the development of the Iberian thermal low with net advection of North African air masses; ENEadv (21%) is especially frequent in spring and summer as a result of a blocking anticyclone over Central Europe that leads to E/NE advection towards the IP. During the winter, the most frequent CTs are the AtlHi (12%) which is an anticyclonic situation that enables the arrival of Atlantic air masses towards the IP and the ZonWadv (10%) which is characterised by zonal Atlantic maritime advection. Finally, WSWadv (10%) is typical of transitional seasons presenting unstable conditions with western-southwestern winds and precipitation.

Following Valverde et al. (2014), one day for each CT was identified as representative of the synoptic scale circulation following an objective procedure (Table 2). On the representative day of each CT, the atmospheric circulation over the IP domain corresponds with the one characterising each CT. This selection of days is used to analyse power plants plume dynamics because the obtained conclusions are representative of the existing synoptic variability over the IP for the present climate (1983–2012).

2.3. Air quality simulations

The CALIOPE-AQFS (www.bsc.es/caliope) operationally provides 48-h forecast concentrations of main pollutants over the IP at high spatial (4 km × 4 km) and temporal resolution (1 h); the system is described

Please cite this article as: Valverde, V., et al., A model-based analysis of SO_2 and NO_2 dynamics from coal-fired power plants under representative synoptic circulation types over the Iberian Peninsula..., Sci Total Environ (2015), http://dx.doi.org/10.1016/j.scitotenv.2015.09.111

Table 1
Characteristics of the coal-fired power plants considered in this study (2009 Data used in HERMESv2).

Power plant/acronym/PRTR register code/altitude (masl)	Installed capacity/production[a]	# stacks and stack height (magl)	Type of fuel	SO_x emissions[a] (Gg year^{-1})	NO_x emissions[a] (Gg year^{-1})
As Pontes/ASP/3536/360	1468 MW/5815 GWh	4 × 356	Brown lignite	4.99	7.46
Aboño/ABO/2928/42	921 MW/4876 GWh	1 × 175 + 1 × 225	Coal + anthracite	5.83	8.13
Compostilla II/COM)/8246/590	1341 MW/2819 GWh	2 × 270 + 2 × 290	Coal + anthracite	3.79	8.38
Guardo/Velilla/GUA/3590/1120	498 MW/980 GWh	1 × 70 + 1 × 176	Coal + anthracite	0.82	3.07
Andorra/AND/3530/612	1101 MW/2717 GWh	3 × 343	Black lignite	11.71	10.00
Litoral de Almería, Carboneras/CAR/3537/13	1159 MW/5804 GWh	2 × 200	Imported coal	13.99	9.80
Los Barrios/LBB/3531/11	568 MW/3219 GWh	1 × 230	Imported coal	2.53	5.39

[a] Based on year 2009.

and evaluated in detail elsewhere (Baldasano et al., 2008, 2011; Pay et al., 2011, 2012, 2014). It integrates the Weather Research and Forecasting model which uses the advanced research dynamical solver, WRF-ARWv3.5 (Skamarock and Klemp, 2008), a specific emission model (HERMESv2; Guevara et al., 2013, 2014), the Eulerian area-limited Community Multi- scale Air Quality model (CMAQv5.0.2; Byun and Schere, 2006), and an off-line mineral dust atmospheric model (BSC-DREAM8bv2 (Pérez et al., 2006a,b; Basart et al., 2012).

WRF-ARW runs over Europe (the mother domain) at 12 km × 12 km horizontal resolution using initial and boundary conditions from the Global Forecast System (GFS/FNL) dataset with 6-h temporal resolution, 0.5° × 0.5° horizontal resolution and 12-h spin-up. Over the IP, WRF runs at 4 km × 4 km using a one-way nesting over the mother domain. Vertically, WRF-ARW is configured with 38 σ vertical levels from the surface up to 50 hPa, with 11 levels characterising the planetary boundary layer (PBL). The Yonsei Univeristy scheme is used to parametrize the PBL.

The CMAQ model uses MOZART4-GEOS5 forecasts as chemical boundary conditions (Lat 1.9° × Lon 2.5°, 6 h). A time-independent vertical concentration profile is used to settle the initial conditions, and a 7-day spin-up is used to heat the model before each simulation. The Meteorology-Chemistry Interface Processor of CMAQ (MCIP) is used to collapse the 38 σ levels of WRF into 15 vertical layers, 12 of which are below 1500 m above ground level (magl). The vertical diffusion module used is the Asymmetric Convective Model Schemev2 whereas the horizontal and vertical advection schemes are the Yamartino mass-conserving and the Piecewise Parabolic Method, respectively.

The HERMESv2 emission model is used for calculating Spanish emissions (Guevara et al., 2013, 2014). For Spanish power plants, HERMESv2 calculates emissions using real facility activity and measured emissions factors from 2009 (OCEM-CIEMAT, personal communication).

Regarding the CALIOPE-AQFS performance, the system is evaluated in near-real time against hourly air quality observations from more than 400 ground-level stations from the Spanish monitoring network. There are also annual evaluations of the system that provide robustness to the results (Baldasano et al., 2011 and its supplementary material; Pay and Baldasano, 2012; Arévalo et al., 2014).

2.4. Plume dynamics characterisation: methods and data

In order to understand the relationship between each CT and the plume dynamics the present analysis takes into account the location, the stack height and the emission rates of each facility, meteorological fields, and SO_2 and NO_2 concentration profiles.

At each power plant, meteorological hourly fields are extracted from the MCIP module. Wind speed, wind direction and vertical vorticity at different vertical layers enable an analysis of horizontal and vertical plume transport close to the power plant. Positive vertical vorticity causes counter clockwise circulation and upward movement of the air mass, whereas negative values cause clockwise circulation and downward movement.

Fig. 1. Topographic map of the Iberian Peninsula and location of the studied coal-fired power plants according to Table 1.

Please cite this article as: Valverde, V., et al., A model-based analysis of SO_2 and NO_2 dynamics from coal-fired power plants under representative synoptic circulation types over the Iberian Peninsula..., Sci Total Environ (2015), http://dx.doi.org/10.1016/j.scitotenv.2015.09.111

Table 2
Representative day of each of the six typical circulation types in 2012.

CT	1983–2012 frequency	2012 frequency	Representative day
NW advection (NWadv)	23.9%	21.9%	Sunday 29/07/2012
Iberian thermal low (IBtl)	22.4%	21.6%	Sunday 19/08/2012
E/NE advection (ENEadv)	21.3%	8.8%	Thursday 24/05/2012
Atlantic high (AtlHi)	12.0%	17.8%	Tuesday 24/01/2012
W/SW advection (WSWadv)	10.4%	20.5%	Tuesday 16/10/2012
Zonal Western advection (ZonWadv)	10.1%	9.3%	Tuesday 03/01/2012

As different plume behaviours are expected when emission occurs under and above the PBL, the PBL height (PBLH, magl) was also analysed using data from the MCIP module. SO_2 and NO_2 hourly concentrations are estimated by the CMAQ model for the representative day of each CT. A zero-out approach (running two equal simulations but setting the emissions from the seven selected facilities to zero in one of them) is used to obtain the contribution of the power plants in terms of air quality concentrations. Two complimentary approaches are considered to analyse these data. On the one hand, N–S and W–E cross-sections up to 3000 m above sea level (masl) passing by the power plant are obtained (daily maximum and hourly concentration are used). Cross-sections plots help characterising the plumes diffusion and their relationship to topography. On the other hand, SO_2 and NO_2 surface concentration maps and total column mass maps allow describing the horizontal plume transport. The plume length (km) is calculated as the maximum distance from the facility that has a surface contribution higher than the remote background concentration (RBC) in Spain. RBC is calculated as 2003–2012 average of 10 Spanish EMEP stations corresponding to 4.3 μg NO_2 m^{-3} and 1.2 μg SO_2 m^{-3}.

3. Results

3.1. Evaluation of CALIOPE

To analyse the performance of the modelling system, the three most widely used statistical indicators according to Dennis et al. (2010) have been computed: the Mean Bias (MB), the Root Mean Squared Error (RMSE) and the correlation coefficient (r). The CALIOPE-AQFS properly reproduces SO_2 and NO_2 concentrations as shown by statistics (Table 3) calculated on an hourly basis for a 4-day episode finishing on the representative day of each CT against validated observations from the Spanish monitoring network (a map with the location of stations used is presented in the Supplementary Material, Fig. S1). The SO_2 and NO_2 concentrations tend to be underestimated; on average for the six CTs, the MB are −2.2 μg SO_2 m^{-3} and −5.6 μg NO_2 m^{-3}. However, the general temporal variability is well captured, with a r-SO_2 = 0.19 and r-NO_2 = 0.58. For SO_2, the lowest error is found for the WSWadv (RMSE = 5.3 μg m^{-3}) and are alike for the other CTs (RMSE ~ 9.5 μg m^{-3}). For NO_2, the highest error is found for the AtlHi (RMSE = 20.1 μg m^{-3}) and lowest is also minimum for the WSWadv episode (RMSE = 15.2 μg m^{-3}).

The DELTA TOOL (Thunis and Cuvelier, 2014) is a harmonised tool that is useful to assess the model quality objectives that indicate the level of accuracy considered to be acceptable for regulatory applications according to the Ambient Air Quality Directive 2008/50/EC (AQD). The DELTA TOOL version 4.0 has been used to evaluate the CALIOPE-AQFS performance for each 4-day episode considering all the available air quality stations regardless their typology. In this tool's version, the SO_2 Target plot is not available because there is no parametrization to estimate SO_2 measurements uncertainty and thus only results for NO_2 are discussed (Fig. 3). For both plots, stations located in the green area fulfil the model quality objectives based on bias, correlation, error, and observation uncertainty. The number of stations fulfilling the target criteria, indicated as a percentage in the plots, ranges from 82% to 94% on all CTs. According to the AQD, the minimum expected performance of a model is 90%. The worst results are obtained for the ENEadv (~87%) and IBtl (~88%) probably related to a combination of high NO_2 emissions together with stagnant conditions over large parts of the IP that make it difficult to properly model the transport dynamics. On the contrary, the best results (>90%) are recorded under Atlantic advection conditions (ZonWadv, WSWadv nd NWadv). Overall, there is a negative bias for surface concentration, especially for low values (<10 μg m^{-3}). Moreover, the target plots highlight that correlation errors dominate over the standard deviation error.

3.2. Emissions characterisation

To explain the power plants' plume dynamics it is necessary to characterise the temporal emissions variability. The power plants emissions depend on the electricity demand and therefore change throughout the year and along the day (the emission rates for each facility along the representative day of each CT are presented as Supplementary Material, Fig. S2). In general terms, the emission rates are the highest during winter CTs AtlHi and ZonWadv, both with a representative day in January 2012. For the seven power plants, the daily emission rate ranges 250–3400 kg SO_2 day^{-1} and 900–2900 kg NO_2 day^{-1}. In ASP however, the maximum rates are reached in NWadv (1310 kg SO_2 day^{-1} and 1960 kg NO_2 day^{-1}). In August, during the IBtl, the emissions are minimal in the seven power plants ranging, 50–2000 kg SO_2 day^{-1} and 190–900 kg NO_2 day^{-1}.

Superimposed to the seasonal variations, the emission rates change following a daily cycle. Emission rates are the lowest at night and rises in the early morning showing their maximum at 12:00. A second maximum is reached at 20:00–21:00. There are larger variations on emission rates along the daily cycle during winter CTs than during summer, especially for power plants with an emission rate lower than 20 kg h^{-1} (GUA, LBB).

3.3. Plume dynamics from Spanish power plants

In this section, the SO_2 and NO_2 plume dynamics are described on the representative day of each CT using i) maps for the daily maximum surface concentration (Fig. 4), ii) maps for the daily maximum total column mass (Fig. 5), iii) cross-sections at the power plants for the daily maximum concentration (Supplementary Material S5) and, iv) daily cycle at the power plant for the hourly PBLH, wind speed and direction and, the vertical vorticity (Supplementary Material S7). The same analysis is shown for NO_2 in the supplementary materials S3, S4, S6 and S7.

3.3.1. NWadv

ASP and ABO, located the Atlantic coast, are reached by N/NW winds along the day (Fig. 2). The plume from ASP reaches 1250 m above injection height (maih, computed as altitude of the facility plus stack height) and it is oriented towards the SE/E (Figs. 4, 5, S3, S4) reaching 125 km for SO_2 and 25 km for NO_2 (Fig. 6). At ABO, the plume is transported southwards (60 km for SO_2 and 50 km for NO_2) attaining ~700 maih. There is a fumigation process occurring at both power plants at midday leading to a maximum increase in surface concentration close to the source (10–15 km) of 7.3 μg SO_2 m^{-3} and 6.5 μg NO_2 m^{-3} in ASP and 14.3 μg SO_2 m^{-3} and 16.4 μg NO_2 m^{-3} in ABO. This fumigation process at noon is related to i) the injection is done within the PBL which height is maximum at midday (ASP ~ 1000 magl, ABO ~ 600 magl) due to thermal heating of the ground (Fig. S7a, b); and ii) between 13:00 and 17:00 the vertical velocity is negative, favouring a vertical transport of the emissions towards the ground. The main difference between ASP and ABO is that in the former, although the emission rates for SO_2 and NO_2 are higher than in ABO, the emissions are injected at higher altitude ($ASP_{injection\_height}$ = 716 masl > ABOinjection_height = 267 masl) favouring a larger pollutants dispersion (in ASP there is little plume formation for NO_2, Fig. S3).

Please cite this article as: Valverde, V., et al., A model-based analysis of SO_2 and NO_2 dynamics from coal-fired power plants under representative synoptic circulation types over the Iberian Peninsula..., Sci Total Environ (2015), http://dx.doi.org/10.1016/j.scitotenv.2015.09.111

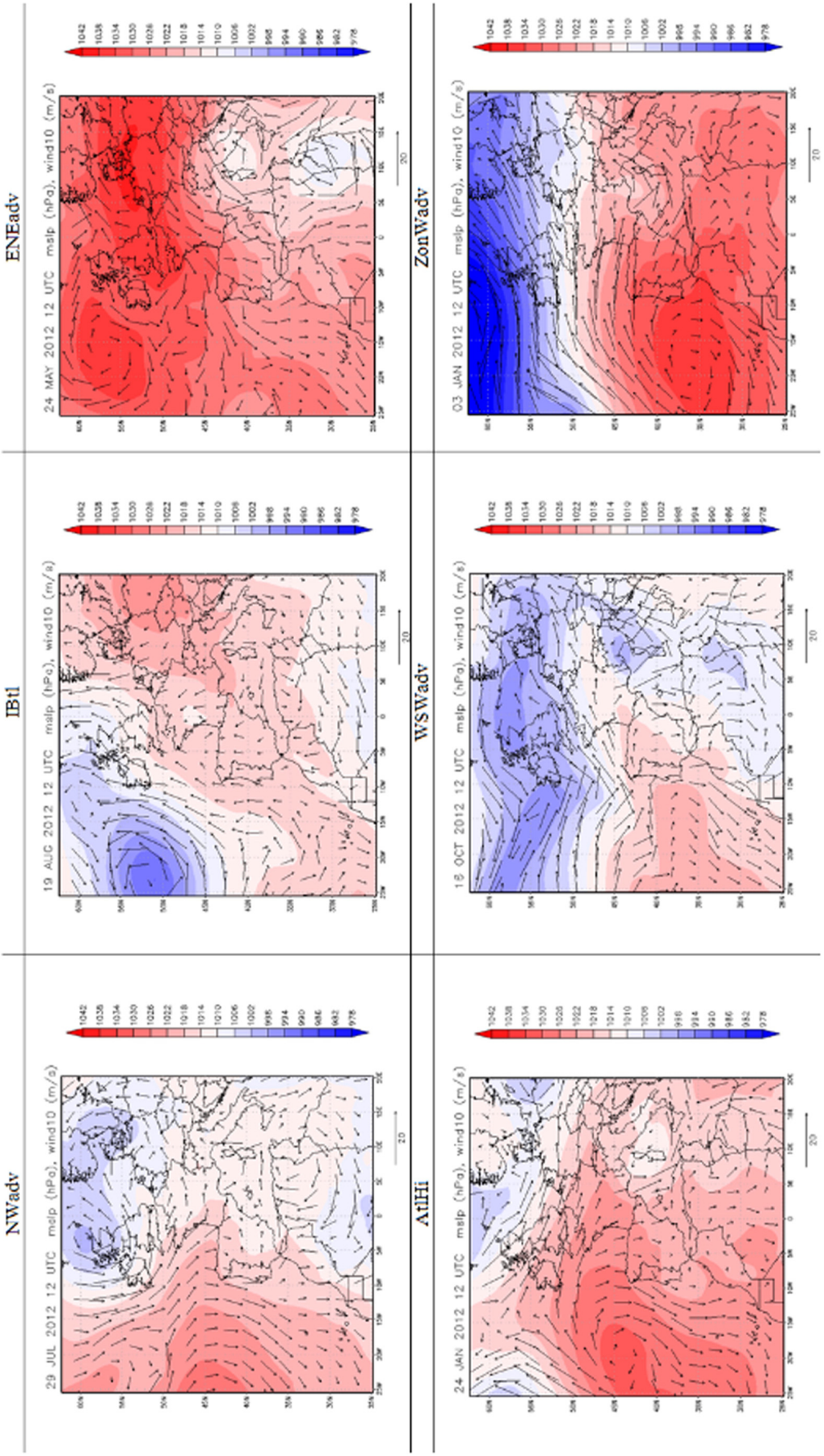

Fig. 2. Mean sea-level pressure (hPa) and 10-m wind ($m\ s^{-1}$) of the representative day of each CT in 2012 (12:00 UTC) over the Iberian Peninsula.

Please cite this article as: Valverde, V., et al., A model-based analysis of SO_2 and NO_2 dynamics from coal-fired power plants under representative synoptic circulation types over the Iberian Peninsula..., Sci Total Environ (2015), http://dx.doi.org/10.1016/j.scitotenv.2015.09.111

Table 3
Evaluation statistics for all available stations during a 4-day episode finishing on the representative day of each CT. Mean Bias (MB μg m^{-3}), Root Mean Square Error (RMSE μg m^{-3}), correlation coefficient (r), average of the observations (OBS) and average of the model (MOD). Note that only stations with more than 75% of the hourly data over the selected period have been considered as defined in the Air Quality Directive.

	NWadv		IBtl		ENEadv		AtlHi		WSWadv		ZonWadv	
	SO_2	NO_2	SO_2	NO_2	SO_2	NO_2	SO_2	NO_2	SO_2	NO_2	SO_2	NO_2
# stations	395	454	402	455	407	458	404	464	394	446	404	465
MB (μg m^{-3})	−1.6	−3.6	−0.9	−2.8	−2.6	−6.9	−2.5	−7.3	−2.2	−4.7	−3.3	−8.2
RMSE (μg m^{-3})	9.8	15.4	10.0	18.6	9.1	16.7	9.4	20.1	5.3	15.2	9.1	18.6
r	0.15	0.47	0.22	0.48	0.26	0.59	0.16	0.63	0.19	0.65	0.17	0.68
OBS (μg m^{-3})	4.4	14.3	4.8	16.3	5.0	16.8	5.6	24.1	3.9	16.3	5.3	21.6
MOD (μg m^{-3})	2.8	10.7	3.9	13.5	2.4	9.9	3.2	16.8	1.8	11.6	2.0	13.4

COM and GUA are located in Northern Spain in areas with complex topography (Fig. 1). The Cantabrian Mountains (2000 masl with W–E orientation) situated to the North of COM and GUA behave as an orographic barrier reducing the influence of the Atlantic Ocean over these areas. Synoptic NW winds towards COM and GUA are transformed into westerlies that blow parallel to the Cantabrian Mountains along the day (Fig. S7c and d) transporting the SO_2 and NO_2 plumes to the E/NE. COM plumes reach ~850 maih and ~75 km for SO_2 and ~55 km for NO_2. The maximum surface contributions are registered at 10 km from the facility and are 6.4 μg SO_2 m^{-3} and 8.6 μg NO_2 m^{-3}. In GUA, the plume of both pollutants attains 400 maih and 25 km. The maximum contribution is disclosed at 7 km from the source (3.7 μg SO_2 m^{-3} and 10.5 μg NO_2 m^{-3}). As in ASP and ABO, in COM and GUA, there is also a fumigation process from 10:00 that explains the pollutants diffusion towards the ground although the PBLH is higher (~1400 magl) than in the Atlantic power plants. The length and width of GUAs plumes is lower than those of COM (Figs. 5, S4) due to a combination of factors: lower SO_2 and NO_2 emission rates at GUA, lower plume altitude (the emissions are less dispersed because they are exposed to weaker winds) and because GUA is under the influence of mountain-valley winds which favour recirculations close to the source (Fig. S7d).

The Ebro valley, where AND is located, connects the Iberian's Peninsula Mediterranean and Atlantic coasts. Under NWadv, northwesterlies are channelled by the Ebro Valley. At night, the wind is oriented down valley towards the Mediterranean Sea (Fig. S7e). However, during the day, the wind is up valley (SE) driven by strong sea–land breezes. Moreover, orographic mountain-valley winds originated in the close Gúdar Mountains (1600 masl, 40 km south of the power plant, Fig. 1) increase wind complexity in the region. The SO_2 and NO_2 plumes from AND drift without a dominant direction during the morning until mesoscale sea breezes are more intense and drive the plumes towards the W/NW (Fig. 5 and S4). The plume reaches 1750 maih for SO_2 and 1350 maih for NO_2. There is a differential behaviour between pollutants due to their different diffusivity in ambient air (the SO_2 and NO_2 diffusivity at 296 K are: 12,532 ± 1733 Pa cm^2 s^{-1} and 14,132 ± 4933 Pa cm^2 s^{-1}, respectively according to Tang et al., 2014). The NO_2 plume does not reach the ground, whereas the SO_2 plume affects first the Arcos Mountains (700 masl, 20 km westward from AND) contributing to 6.1 μg SO_2 m^{-3} and is further transported up to 100 km from the source.

Under NWadv, CAR is reached by easterlies during night hours transporting the plume towards the sea (SE). However, during the day, mesoscale sea–land breezes drive wind dynamics at surface and at injection height (Fig. S7f) carrying the pollutants inland (W/SW) at 800 maih for SO_2 (Fig. S5f) and up to 500 maih for NO_2 (Fig. S6f). The emissions are injected above the PBL ($PBLH_{max}$ < 300 magl) favouring its horizontal transport: the SO_2 plume reaches 150 km and the NO_2 30 km. This difference in the maximum plume length between the two pollutants is caused by the large SO_2 emission rate in the fuel used in CAR (Fig. S2). Moreover, the SO_2 plume affects the Alhamilla Mountains (1300 masl, ~30 km from the power plant, Fig. S5f) contributing with 11.4 μg SO_2 m^{-3} to the surface concentration.

The Strait of Gibraltar is a complex topographic region that receives Mediterranean and Atlantic influences. In this region, NWadv is characterised by western synoptic winds (Fig. 2). However, the SO_2 and NO_2 plumes from LBB are transported to the E during the early morning and around 9:00–10:00 there is a shift in wind direction (Fig. S7g) and E/SE winds drive the plume towards the NW (~50 km, at 600 maih). During the shift in the advection direction, negative vertical vorticity is registered at LBB favouring a fumigation process. The eastern façade of the Algeciras Mountains (Fig. 1, 15 km from the source) is reached by the plumes of LBB contributing to 10.6 μg SO_2 m^{-3} and 15.0 μg NO_2 m^{-3} to surface concentration. It is also noteworthy that from 20:00 the PBLH is <35 magl. This nocturnal layer enhances the concentration of pollutants at surface level.

3.3.2. IBtl

Under IBtl, the North-Western Iberian Peninsula is under the cyclonic influence of the Icelandic Low (Fig. 2). The emissions at ASP are the lowest of all the representative days (30 kg SO_2 h^{-1} and 40 kg NO_2 h^{-1}), which hinders the formation of distinctive plumes. Although the PBLH at midday is ~1000 magl (Fig. S7a) and the injection is done within the PBL, there is positive vertical vorticity during this timespan (11:00–14:00), which prevents fumigation towards the ground.

The Cantabrian Mountains disconnect ABO from the southwards synoptic advection affecting the IP. Plume dynamics in ABO are driven by a mesoscale vortex that favours sea–land dispersion during the day and land–sea during the night at 500 maih (Figs. S5b and S6b). The emissions are injected above the PBL (~400 magl) which favours its horizontal transport. The SO_2 and NO_2 plumes contact the ground at 95 and 25 km from the source, respectively. The contribution from the power plant in terms of surface concentration is maximal at 18 km south of the facility (<5 μg m^{-3} for SO_2 and NO_2).

Inland the IP, during the summer IBtl, the PBL reaches its maximum in COM (~1900 magl), GUA (~2000 magl) and AND (~2100 magl). Although the emissions at midday are injected within the PBL in these three facilities, there is little transport towards the ground. This is due to i) the SO_2 and NO_2 emission rates are the lowest of all the CTs (Fig. S2) due to lower electricity demand and ii) the vertical vorticity at midday is mainly positive due to soil heating. The maximum surface contribution occurs in COM at 7 km from the source: 4.7 μg SO_2 m^{-3} and 6 μg NO_2 m^{-3}. Considering the total column, the SO_2 and NO_2 plumes from COM and GUA are driven by southerlies northwards towards the Cantabrian Mountains that are a topographic block that avoids longer dispersion (Figs. 5 and S4). At AND, the winds are weak without dominant direction enabling that AND plumes remain close to the point source and reach 1500 maih for SO_2 and 1000 maih for NO_2.

At CAR, the wind blows from the E/NE along the day (Fig. S7f). In LBB, however, the wind is from the E (Fig. S7g). The plumes of CAR are transported in altitude 680 maih for SO_2, 380 maih for NO_2 (difference due to the larger SO_2 than NO_2 emission rate in CAR) towards the SW (Figs. 5 and S4) whereas in LBB, the plume is oriented to the W reaching 360 maih for both pollutants. In both cases, the injection is done above the PBL favouring its horizontal transport. The SO_2 plumes from CAR and LBB have a maximum length of 97 and 81 km from the source, respectively.

Please cite this article as: Valverde, V., et al., A model-based analysis of SO_2 and NO_2 dynamics from coal-fired power plants under representative synoptic circulation types over the Iberian Peninsula..., Sci Total Environ (2015), http://dx.doi.org/10.1016/j.scitotenv.2015.09.111

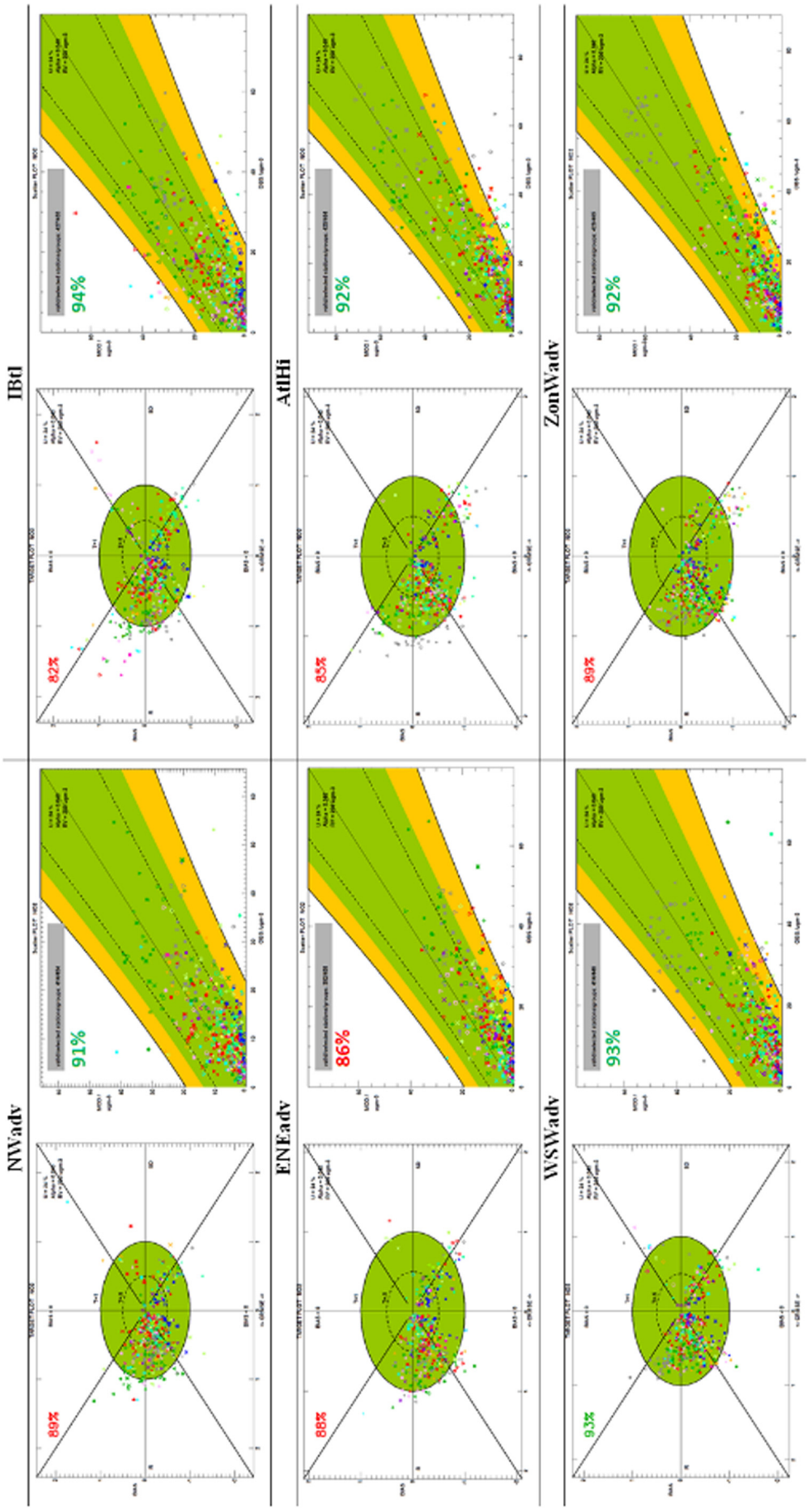

Fig. 3. Target plot (left) and scatter diagram plot (right) from DELTA TOOL for hourly pairs of observed-modelled NO_2 concentration along a 4-day episode of each CT in 2012. Symbols and colours represent the different stations Percentage indicates stations fulfilling the model quality objective target criteria.

Please cite this article as: Valverde, V., et al., A model-based analysis of SO_2 and NO_2 dynamics from coal-fired power plants under representative synoptic circulation types over the Iberian Peninsula..., Sci Total Environ (2015), http://dx.doi.org/10.1016/j.scitotenv.2015.09.111

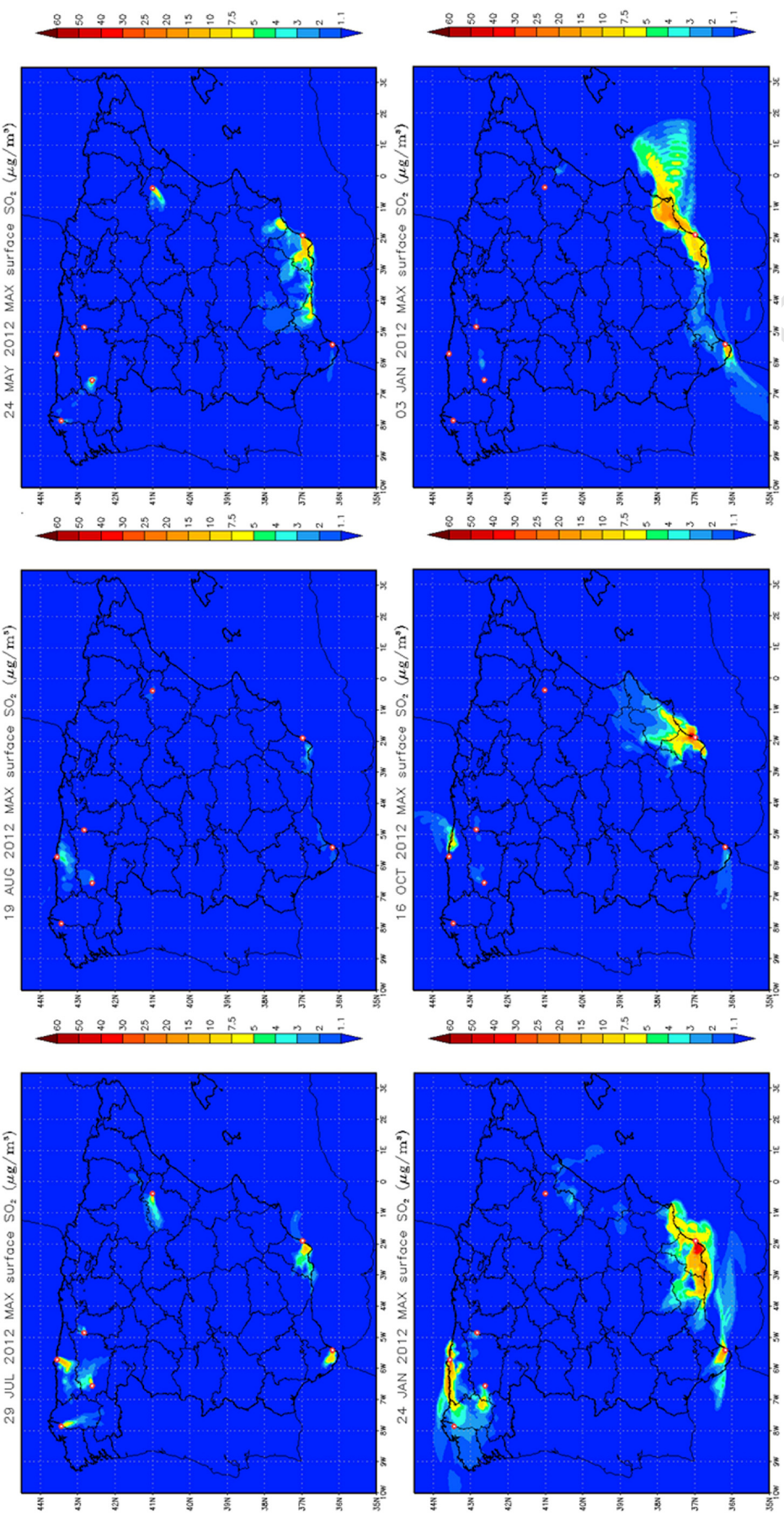

Fig. 4. Daily maximum SO_2 surface concentration ($\mu g\ m^{-3}$) associated to the emissions in the seven analysed power plants on the representative day of each CT.

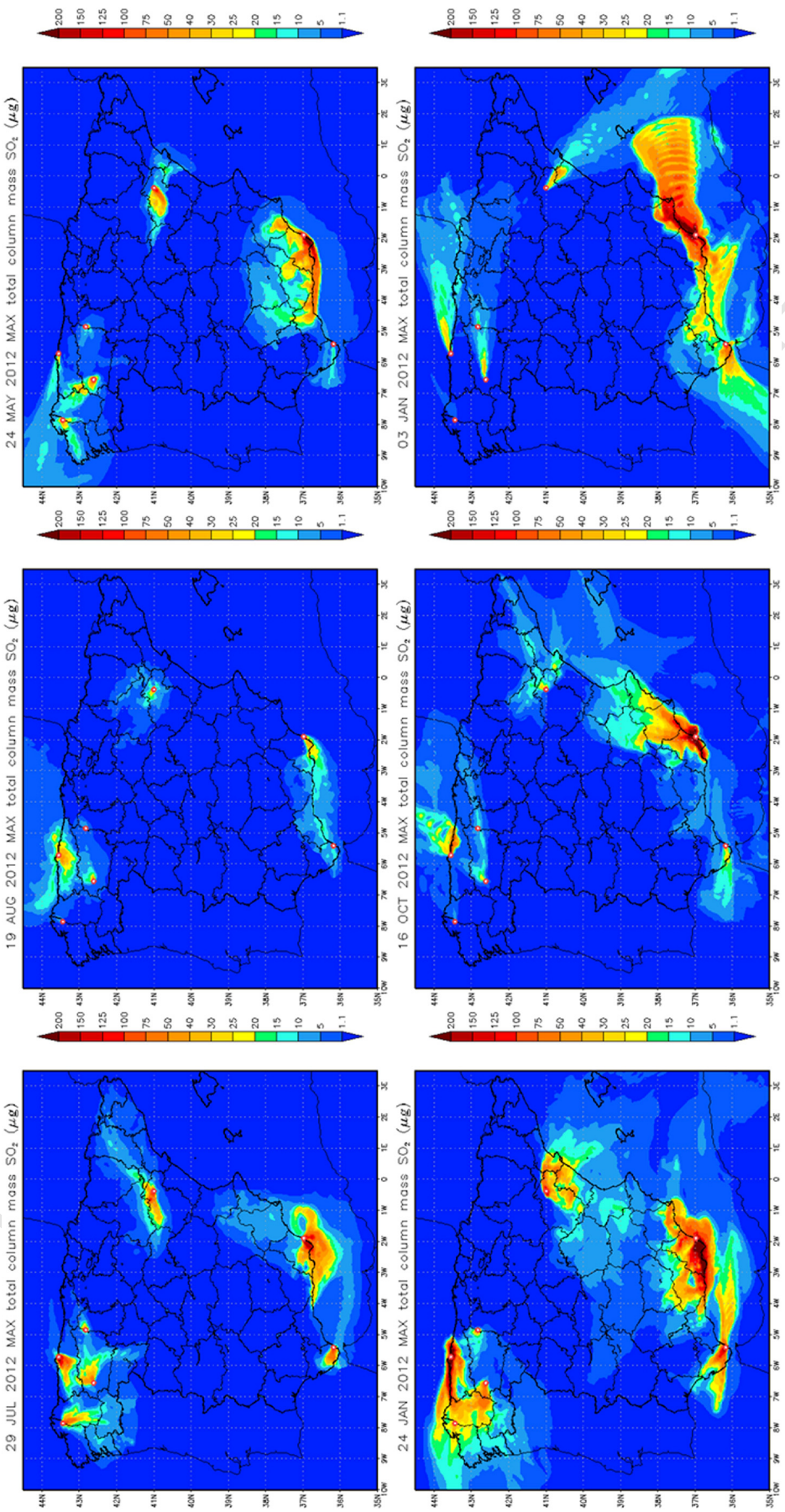

Fig. 5. Daily maximum SO_2 total column mass (μg) associated to the emissions in the seven analysed power plants on the representative day of each CT.

Please cite this article as: Valverde, V., et al., A model-based analysis of SO_2 and NO_2 dynamics from coal-fired power plants under representative synoptic circulation types over the Iberian Peninsula..., Sci Total Environ (2015), http://dx.doi.org/10.1016/j.scitotenv.2015.09.111

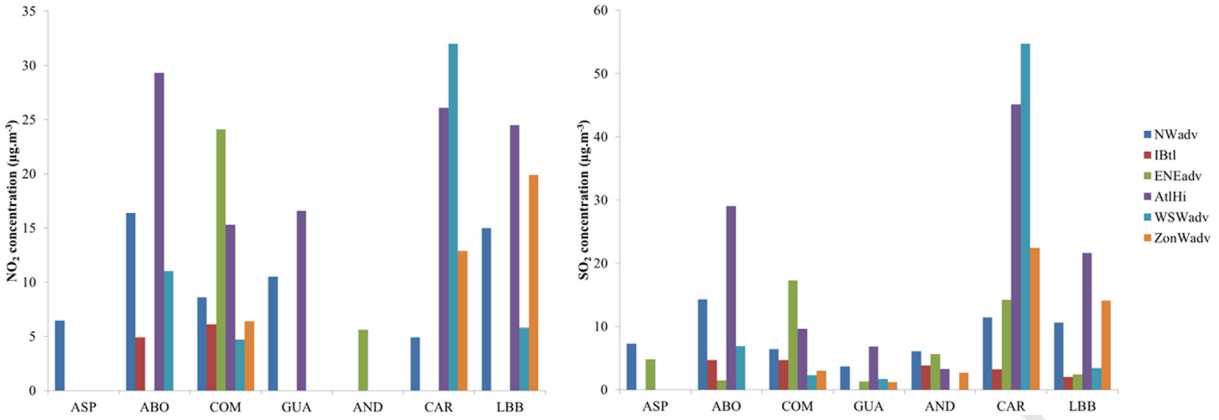

Fig. 6. Daily maximum NO_2 (left) and SO_2 (right) contribution to surface concentration (μg m^{-3}) for the seven power plants under each CT. Different scales apply.

3.3.3. ENEadv

The blocking anticyclone over Central Europe that characterises ENEadv leads to the arrival of easterlies towards ASP, ABO, COM and GUA. However, this general advective pattern is modulated by the Cantabrian Mountains. Winds arriving at ASP are from the SE/E during 00:00–12:00 and from NE/E from 15:00 onwards (Fig. S7a). The plumes from ASP are transported northwards during the morning (at 1200 maih) and after the change in wind direction, the plumes go towards the SW/S (Fig. 5 and S4). At midday, the injection is done within the PBL favouring fumigation towards the ground (<5 μg m^{-3} for both pollutants).

In ABO, the advection is from the E, parallel to the coastline at surface and at the injection height (Fig. S7b). For both pollutants, the plume is oriented towards the W at 230 maih (Figs. 5 and S4). The injection is done above the PBL along the day. This hinders the fumigation towards the ground and favours the horizontal transport (SO_2 plume length is 59 km whereas the NO_2 does not even reach the ground.

The easterlies arriving at COM drive the SO_2 and NO_2 plumes towards the W/NW. However, there is little horizontal plume advection (Figs. 4 and S3). The plume dynamics are dominated by the vertical vorticity (the maximum plume altitude is >1500 maih). At midday negative vorticity combined with emission injection within the PBL ($PBLH_{max}$ = 1800 magl) enhances fumigation towards the ground, close to the source. The maximum contributions to surface concentrations occur at 3.5 km from the source and attain 17.3 μg SO_2 m^{-3} and 24.1 μg NO_2 m^{-3}. GUA plumes are also transported to the W without affecting the ground at 300 maih (Figs. S5d and S6d).

The advection under ENEadv at AND is from the North channelled by the Ebro valley (Fig. 2). The simulation shows a complex situation with a superposition of the synoptic northerlies, sea–land breezes from the Mediterranean and downslope winds from the Gúdar Mountains (Fig. S7e). The plumes from AND are transported to the SE during the morning (maximum altitude: 1350 maih for SO_2 and 1050 for NO_2). At midday with the development of sea–land breezes, the plumes turn westwards and are oriented towards the SW from the facility (Figs. 5 and S4). The change in wind direction at midday at AND together with negative vertical vorticity and emission injection within the PBL ($PBLH_{max}$ ~ 1800 magl) enables a fumigation process. The maximum contribution to surface concentration is at 9 km from AND (5.6 μg SO_2 m^{-3} and 5.6 μg NO_2 m^{-3}).

In Southern Spain, the ENEadv is characterised by easterlies (Fig. 2). The CAR plumes are transported towards the SW and W with a maximum altitude of ~800 maih. As the emission is done above the PBL ($PBLH_{max}$ < 200 magl, Fig. S7f) the horizontal transport is enhanced enabling long plumes up to 200 km away from the stack (Figs. 5 and S4). It is noteworthy that the marine boundary layer is a barrier to the vertical movement of the plume favouring the transport of the pollutants inland. The plume affects the ground when it reaches the nearby Alhamilla Mountains, W of CAR (Figs. S5f and S6f) with up to 14.2 μg SO_2 m^{-3} and 7.5 μg NO_2 m^{-3}.

In LBB the plumes are transported westwards (~100 km) close to the ground (~200 maih). The maximum contribution to surface concentration is 2.4 μg SO_2 m^{-3} and 20 μg SO_2 m^{-3} over the Algeciras Mountains, 20 km W of the source. The difference between pollutants is due to the emission rates (10 kg SO_2 h^{-1} and 20 kg NO_2 h^{-1}). Moreover, during the night hours, there is a nocturnal layer (PBLH is <50 magl) that increases surface concentration close the source (Fig. S7g).

3.3.4. AtlHi

Under the winter AtlHi there is a low PBLH at the seven power plants locations (PBLH <500 magl). This fact enables that the emission injection occurs above the PBL favouring their dispersion. On the other hand, AtlHi together with ZonWadv are the CTs characterised by highest emission rates (Fig. S2).

On the Cantabrian coast, AtlHi advection is depicted by northerlies that turn westwards when reaching the coastline. The plumes from ASP are transported westwards reaching ~1100–1200 maih without contacting the surface. The region of ASP is affected by quick easterlies coming from Asturias transporting SO_2 and SO_2 concentrations from ABO along the surface (Figs. S5a and S6a). In ABO, the plumes are parallel to the Atlantic coast (E–W orientation) and reach long distances (268 km for SO_2 and 204 km for NO_2) because there are not topographic barriers that stop them (0–600 maih, Figs. S5b and S6b). The highest contributions to surface concentration from ABO occur within 23 km from the source (~29 μg m^{-3} for both pollutants). The high emission rates together with high dispersive conditions favour the formation of wide multi-source plumes on North-Western IP during AtlHi (Fig. 5 and S4).

The COM plumes are also oriented westwards but the transport is partially stopped by the Galician Mountains (40 km to the W) affecting the surface concentration in that area (Figs. S5c and S6c, 9.6 μg SO_2 m^{-3} and 15.3 μg NO_2 m^{-3}). The plumes from COM have a length of ~100 km and a maximum altitude of ~1100 maih. In COM and ABO, the PBL is very close to the ground (PBLH <50 magl) during the night, enhancing the concentration of the pollutants at the surface (Fig. S7b and c).

During the day, the plume from GUA is transported towards the W (27 km, ~500 maih for NO_2 and ~700 maih for SO_2). However, the nocturnal downslope winds from the nearby mountains drive the plume towards the S (Figs. S5d and S6d). At midday (12:00–15:00) the PBLH is high enough (~500 magl) to enable the emission injection within the PBL favouring the increase of surface concentration close to the source (<3 km, 6.8 μg SO_2 m^{-3} and 16.6 μg NO_2 m^{-3}).

Under AtlHi, the northern advection towards AND is channelled by the Ebro valley (Fig. 2) driving the plumes down valley towards the

Please cite this article as: Valverde, V., et al., A model-based analysis of SO_2 and NO_2 dynamics from coal-fired power plants under representative synoptic circulation types over the Iberian Peninsula..., Sci Total Environ (2015), http://dx.doi.org/10.1016/j.scitotenv.2015.09.111

SE/E (Figs. S5e and S6e) at 1650 maih for SO_2 and 1150 maih for NO_2. The differential diffusivity of the pollutants explains this difference in altitude. The plumes reach 130–140 km from the source and the contribute little to surface concentrations (<4 μg m^{-3}).

Westerlies are characteristic of the AtlHi on the Strait of Gibraltar as well over the Alboran Sea (Fig. 2). However, winds blow from the NE in CAR (Fig. S7f) showing a complete disconnection from the main synoptic advection caused by an anticyclonic eddy located on the Mediterranean, 60 km away from the coastline. The plumes from CAR are transported to the SW/W. The Alhamilla Mountains blocks the progress of the plume westwards and enhances the concentration of pollutants on its eastern side 15–20 km from the source (45.1 μg SO_2 m^{-3} and 26.1 μg NO_2 m^{-3}; Figs. S4f and S5fb). The SO_2 and NO_2 plumes reach 2800 maih and 1200 maih and up to 250 and 180 km away from the source, respectively.

The plume from LBB is driven by westerlies into the Mediterranean during the morning (00:00–10:00). However, at midday there is a change in wind direction (E advection) and the LBB plume is transported towards the W (~180 km and 500–600 maih). When the wind changes its main direction there is a significant diffusion of SO_2 and NO_2 from the stack to the ground at midday that contributes up to 21.6 and 24.5 μg m^{-3}., respectively.

3.3.5. WSWadv and ZonWadv

In ASP the wind fields of WSWadv and ZonWadv are similar with a dominant SW surface advection coming from the Atlantic Ocean. However, at the injection height, ZonWadv presents clear western advection whereas under WSWadv, the advection is from the SW (Fig. S7a). High wind speed at the facility on both days together with emission injection above the PBL favours their horizontal dispersion towards the E/NE (Figs. 5 and S3) without attaining the surface in any moment.

Under WSWadv, the SW winds at ABO lead to a NE/N transport of the plumes at ~400 maih towards the Ocean reaching 160 km for SO_2 and 110 for NO_2. The ABO contribution to surface concentration occurs at ~40 km east of the source (6.9 μg SO_2 m^{-3} and 11.0 μg NO_2 m^{-3}). On the other hand, under ZonWadv westerlies disperse the plume towards the E at a maximum altitude of ~400 maih without affecting the surface (Figs. S5b and S6b).

The synoptic winds that characterise WSWadv reach COM and GUA from the SW. The plumes are driven towards the NE at an altitude that ranges 300–500 maih and are stopped by the southern façade of the Cantabrian Mountains (contributing with <5 μg m^{-3} for both pollutants, 20–30 km from the sources). Under ZonWadv, W winds are faster than at WSWadv, both at surface and along the column (Fig. S7c and d) driving the plumes of COM and GUA towards the E without affecting the surface (Figs. 4 and S3).

In AND, under WSWadv the horizontal plume dynamics are a combination synoptic advection and mesoscale breezes (Fig. S7e). During the night the plumes are driven by northwesterlies towards the S however during the day sea–land breezes dominate, leading to a N/NE transport at a maximum altitude of 1650 maih for SO_2 and 1050 for NO_2. Under ZonWadv the westerlies are channelled by the Ebro Valley driving the plumes down-valley going beyond the Mediterranean coastline without affecting the surface (Figs. 5 and S4).

The simulated wind field at CAR shows a complex behaviour. Under WSWadv the sea–land breezes together with an anticyclonic vortex located over the Alboran Sea drive the CAR plumes towards the NE during the morning, towards the N at midday and towards the W in the afternoon (Fig. S6f). This CT is characterised by atmospheric instability with negative vertical vorticity that enhances the fumigation of the plume. The maximum contribution to surface concentration is reached at 4–6 km from the source (54.7 μg SO_2 m^{-3} and 32.0 μg NO_2 m^{-3}). Furthermore, the SO_2 plume is transported up to 290 km from CAR (at an altitude of 1300 maih) and the NO_2 plume reaches 50 km (700 maih). Under ZonWadv, sea breezes are coupled with synoptic westerlies driving the plumes towards the NE, parallel to the coastline from surface up to 800–1200 maih (Figs. S5f and S6f). The strong wind speed at the surface (15–20 m s^{-1}) and over the column that characterise the ZonWadv, favour the formation of long plumes (>250 km). The maximum contribution to surface concentration (22.4 μg SO_2 m^{-3} and 12.9 μg NO_2 m^{-3}) is reached far away from the source (66 km for SO_2 and 116 km for NO_2).

Despite the Atlantic advection that affects the IP under WSWadv and ZonWadv, the area of the Strait of Gibraltar is disconnected from this general pattern and it is dominated by Mediterranean winds under both CTs. The SO_2 plumes from LBB, driven by easterlies at surface and at injection height, reach 170 km and 250 km W of the source at 260 maih and 560 maih for WSWadv and ZonWadv, respectively (Figs. S5g and S6g). The NO_2 plumes share the same transport pattern but they are shorter (55 and 85 km, respectively). The main difference between WSWadv and ZonWadv at LBB is that the emission rates during the latter (22 kg SO_2 h^{-1} and 48 kg NO_2 h^{-1}) duplicate those of WSWadv (11 kg SO_2 h^{-1} and 24 kg NO_2 h^{-1}) leading to a larger contribution at surface level (14.1 μg SO_2 m^{-3} and 19.9 μg NO_2 m^{-3}) over the eastern Algeciras Mountains façade.

4. Conclusions

The CALIOPE-AQFS, used with a zero-out approach, is useful to characterise Spanish coal-fired power plants' SO_2 and NO_2 plume dynamics under representative synoptic circulation types (CTs), and to quantify their contribution to air quality concentrations.

The plume dynamics of the power plants located on the Atlantic Iberian Peninsula (ASP, ABO and COM) are mainly driven by the advective pattern associated to each CT. However, the plumes from AND, CAR and LBB, located over the Mediterranean coast, are driven by a combination of the synoptic advection and mesoscale processes, namely sea–land breezes and wind-channelling by river valleys. The GUA plumes follows the synoptic advection under IBtl, ENEadv, WSWadv and ZonWadv however under NWadv and AtlHi, mesoscale winds related to its complex topographic context (valley drainage) influence the horizontal plume motions.

On average for the seven facilities and six CTs, the maximum plume lengths are 230 km for SO_2 and 112 km for NO_2 (with plumes up to 250–300 km for SO_2 and 200–250 km for NO_2). The average SO_2/NO_2 plume length for CTs characterised by Atlantic advection (NWadv, AtlHi, WSWadv and ZonWadv) is 110/54 km whereas for CTs with non-Atlantic advection (IBtl and ENEadv), the SO_2/NO_2 plume length is 66/6 km. The high coal-fired power plants stack height (70–356 magl), which enable an injection of the emissions at high altitude where the atmosphere is more dispersive, explain these remarkable plume lengths.

The power plant contributions to SO_2 and NO_2 surface concentration occur mainly close to the source (<20 km). On average for the six CTs, the contributions range 2–25 μg SO_2 m^{-3} and 1–15 μg NO_2 m^{-3}. The largest contributions are registered in CAR (25 μg SO_2 m^{-3}, 15 μg NO_2 m^{-3}), ABO (9 μg SO_2 m^{-3}, 14 μg NO_2 m^{-3}), and LBB (9 μg SO_2 m^{-3}, 10 μg NO_2 m^{-3}) whereas the lowest occur in ASP and AND (<5 μg SO_2 m^{-3}, 1 μg NO_2 m^{-3}), the power plants with higher stack heights. The stack height also explains why ASP and AND plumes reach higher altitudes than those of the other facilities. The contributions are more significant when the emissions are injected within the PBL enabling fumigation processes, usually at midday. When the injection occurs above the PBL, horizontal plume dispersion is favoured. However, if the emission rates are low, even when the meteorological conditions favour vertical diffusion, the pollutants are dispersed horizontally.

Within Eulerian photochemical models, the proper simulation of surface pollutant concentration has been related to the accurate determination of PBLH and vertical diffusion (Athanassiadis et al. 2002; Byun et al., 2007). The WRF models the PBL following the Yonsei Univeristy parametrization although it is not clear which PBL scheme performs best for the Iberian Peninsula (Banks et al., 2015). Moreover,

Please cite this article as: Valverde, V., et al., A model-based analysis of SO_2 and NO_2 dynamics from coal-fired power plants under representative synoptic circulation types over the Iberian Peninsula..., Sci Total Environ (2015), http://dx.doi.org/10.1016/j.scitotenv.2015.09.111

the CMAQ models the diffusion using the ACM2 scheme which tends to predict smaller concentrations of primary pollutants at the surface (Pleim, 2007). Considering these modelling uncertainties the described fumigation dynamics have to be taken with caution.

The plume dynamics for each power plant under the six CTs shows similar patterns for SO_2 and NO_2. However, the absolute values of plume length, altitude and contribution to surface concentration differ depending on the emission rates (that are type-fuel dependent) and on the pollutant diffusivity in the air (higher for NO_2 than SO_2). Differences in SO_2 and NO_2 deposition velocity need to be studied to further explain the dissimilarities in their plume dynamics.

The obtained results over the Iberian Peninsula confirm that the pollution dynamics associated to coal-fired power plants depend on a combination of interlinked variables: location and topographic characteristics, stack height, emission rates, and synoptic and mesoscale meteorology.

Uncited references

CALIOPE, n.d
OCEM-CIEMAT, 2015

Acknowledgements

All simulations were performed on the MareNostrum supercomputer hosted by the Barcelona Supercomputing Center. This work is partially funded by the Iberdrola Foundation by the pre-doctoral grant held by V. Valverde, and the post-doctoral grant held by M.T. Pay in the Beatriu de Pinós programme (2011 BP-A 00427), the CICYT project CGL2013-46736-R, and the Severo Ochoa Programme awarded by the Spanish Government (SEV-2011-00067). The authors declare that there are no conflicts of interest.

Appendix A. Supplementary data

Supplementary data to this article can be found online at http://dx.doi.org/10.1016/j.scitotenv.2015.09.111.

References

Arévalo, G., Baldasano, J.M., Pay, M.T., 2014. Evaluación del sistema de pronóstico de calidad del aire CALIOPE en España para el año 2013 (92 pp. Available at: http://www.bsc.es/projects/earthscience/visor/bases_datos/image_viewer/docs/20140513_Informe_Evaluacion_Pronostico_CALIOPE_2013.pdf).

Athanassiadis, G.A., Trivikrama-Rao, S., Ku, J.Y., Clark, R.D., 2002. Boundary layer evolution and its influence on ground-level ozone concentrations. Environ. Fluid Mech. 2, 339–357. http://dx.doi.org/10.1023/A:1020456018087.

Baldasano, J.M., Jiménez-Guerrero, P., Jorba, O., Pérez, C., López, E., Güereca, P., Martin, F., García-Vivanco, M., Palomino, I., Querol, X., Pandolfi, M., Sanz, M.J., Diéguez, J.J., 2008. CALIOPE: an operational air quality forecasting system for the Iberian Peninsula, Balearic Islands and Canary Islands. First annual evaluation and ongoing developments. Adv. Sci. Res. 2, 89–98. http://dx.doi.org/10.5194/asr-2-89-2008.

Baldasano, J.M., Pay, M.T., Jorba, O., Gassó, S., Jiménez-Guerrero, P., 2011. An annual assessment of air quality with the CALIOPE modeling system over Spain. Sci. Total Environ. 409, 2163–2178. http://dx.doi.org/10.1016/j.scitotenv.2011.01.041.

Baldasano, J.M., Soret, A., Guevara, M., Martínez, F., Gassó, S., 2014. Integrated assessment of air pollution using observations and modelling in Santa Cruz de Tenerife (Canary Islands). Sci. Total Environ. 473–474, 576–588. http://dx.doi.org/10.1016/j.scitotenv.2013.12.062.

Banks, R.F., Tiana-Alsina, J., Rocadenbosch, F., Baldasano, J.M., 2015. Performance evaluation of the boundary layer height from lidar and the Weather Research and Forecasting model at an urban coastal site in the north-east Iberian Peninsula. Bound.-Layer Meteorol. http://dx.doi.org/10.1007/s10546-015-0056-2.

Barry, R.G., Perry, A.H., 1974. Synoptic climatology — methods and applications. Weather 29, 195. http://dx.doi.org/10.1002/j.1477-8696.1974.tb07430.x.

Basart, S., Pérez, C., Nickovic, S., Cuevas, E., Baldasano, J.M., 2012. Development and evaluation of the BSC-DREAM8b dust regional model over Northern Africa, the Mediterranean and the Middle East. Tellus Ser. B Chem. Phys. Meteorol. **64**, 1–12. http://dx.doi.org/10.3402/tellusb.v64i0.18539.

Beck, C., Philipp, A., 2010. Evaluation and comparison of circulation type classifications for the European domain. Phys. Chem. Earth A/B/C 35, 374–387. http://dx.doi.org/10.1016/j.pce.2010.01.001.

Brunekreef, B., Holgate, S.T., 2002. Air pollution and health. Lancet 360, 1233–1242.

Byun, D.W., Schere, K.L., 2006. Review of the governing equations, computational algorithms and other components of the Models-3 Community Multiscale Air Quality (CMAQ) Modeling System. Appl. Mech. Rev. 59, 51–77. http://dx.doi.org/10.1115/1.2128636.

Byun, D.W., Kim, S.T., Kim, S.B., 2007. Evaluation of air quality models for the simulation of a high ozone episode in the Houston metropolitan area. Atmos. Environ. 41, 837–853. http://dx.doi.org/10.1016/j.atmosenv.2006.08.038.

CALIOPE Air Quality Forecasting System Website: www.bsc.es/caliope

De Pablo, F., Tomás, C., Rivas Soriano, L., Diego, L., 2008. Winter circulation weather types and hospital admissions for cardiovascular, respiratory and digestive diseases in Salamanca, Spain. Int. J. Climatol. 29, 1692–1703. http://dx.doi.org/10.1002/joc.1802.

De Pablo, F., Rivas Soriano, L., Sánchez Llorente, J.M., Nájera, L.A., 2013. Effects of weather types on hospital admissions for respiratory diseases in Castilla–La Mancha, Spain. Atmosfera 26, 95–107.

De Vries, W., Dobbertin, M.H., Solberg, S., van Dobben, H.F., Schaub, M., 2014. Impacts of acid deposition, ozone exposure and weather conditions on forest ecosystems in Europe: an overview. Plant Soil 380, 1–45. http://dx.doi.org/10.1007/s11104-014-2056-2.

Dennis, R., Fox, T., Fuentes, M., Gilliland, A., Hanna, S., Hogrofe, C., Irwin, J., Trivikrama, R., Scheffe, R., Schere, K., Steyn, D., Venkatram, A., 2010. A framework for evaluating regional-scale numerical photochemical modeling systems. Environ. Fluid Mech. 10, 417–489. http://dx.doi.org/10.1007/s10652-009-9163-2.

Guevara, M., Martínez, F., Arévalo, G., Gassó, S., Baldasano, J.M., 2013. An improved system for modelling Spanish emissions: HERMESv2.0. Atmos. Environ. 81, 209–221. http://dx.doi.org/10.1016/j.atmosenv.2013.08.053.

Guevara, M., Pay, M.T., Martínez, F., Soret, A., Denier van der Gon, H.A.C., Baldasano, J.M., 2014. Inter-comparison between HERMESv2.0 and TNO-MACC-II emission data using the CALIOPE air quality system (Spain). Atmos. Environ. 98, 134–145. http://dx.doi.org/10.1016/j.atmosenv.2014.08.067.

Gurjar, B.R., Jain, A., Sharma, A., Agarwal, A., Gupta, P., Nagpure, A.S., Lelieveld, J., 2010. Human health risks in megacities due to air pollution. Atmos. Environ. 44, 4606–4613. http://dx.doi.org/10.1016/j.atmosenv.2010.08.011.

Hernández, J.F., Cremades, L., Baldasano, J.M., 1995. Dispersion modelling of a tall stack plume in the Spanish Mediterranean Coast by a particle model. Atmos. Environ. 29, 1331–1341. http://dx.doi.org/10.1016/1352-2310(94)00346-M.

Hernández, J.F., Cremades, L., Baldasano, J.M., 1997. Simulation of tracer dispersión from elevated and surface releases in complex terrain. Atmos. Environ. 31, 2337–2348. http://dx.doi.org/10.1016/S1352-2310(97)00027-7.

Jamason, P.F., Kalkstein, L.S., Gergen, P.J., 1997. A synoptic evaluation of asthma hospital admissions in New York City. Am. J. Respir. Crit. Care Med. 156, 1781–1788.

Kassomenos, P.A., Flocas, H.A., Lykoudis, S., Skouloudis, A., 1998. Spatial and temporal characteristics of the relationship between air quality status and mesoscale circulation over an urban Mediterranean basin. Sci. Total Environ. 217, 37–57. http://dx.doi.org/10.1016/S0048-9697(98)00167-3.

MAGRAMA, 2014. Inventarios Nacionales de Emisiones a la Atmósfera 1990–2012. Volumen 2: Análisis por Actividades SNAP. 110 pp. Capítulo 1: combustión en la producción y transformación de energía Available at: http://www.magrama.gob.es/es/calidad-y-evaluacion-ambiental/temas/sistema-espanol-de-inventario-sei-/01_Combusti%C3%B3n_en_la_producci%C3%B3n_y_transformaci%C3%B3n_de_energ%C3%ADa_-_VNC_tcm7-219781.pdf.

Menut, L., Flamant, C., Pelon, J., 1999. Evidence of interaction between synoptic and local scales in the surface layer over the Paris area. Bound.-Layer Meteorol. 93, 269–286. http://dx.doi.org/10.1023/A:1002013631786.

Morabito, M., Crisci, A., Grifoni, D., Orlandini, S., Cecchi, L., Bacci, L., Modesti, P.A., Gensini, G.F., Maracchi, G., 2006. Winter air-mass-based synoptic climatological approach and hospital admissions for myocardial infarction in Florence, Italy. Environ. Res. 102, 52–60. http://dx.doi.org/10.1016/j.envres.2005.12.007.

OCEM-CIEMAT: Oficina para el Control de las Emisiones de las Grandes Instalaciones de Combustión (OCEM), Centro de Investigaciones Energéticas, Medioambientales y Tecnológicas (CIEMAT). Spanish National Office of Emission Control for Large Combustion Facilities.

ORDEN PRE/77/2008, de 17 de enero, por la que se da publicidad al Acuerdo de Consejo de Ministros por el que se aprueba el Plan Nacional de Reducción de Emisiones de las Grandes Instalaciones de Combustión existentes. Available at: http://www.boe.es/boe/dias/2008/01/28/pdfs/A05061-05090.pdf

Palau, J.L., Pérez-Landa, G., Diéguez, J.J., Monter, C., Millán, M., 2005. The importance of meteorological scales to forecast air pollution scenarios on coastal complex terrain. Atmos. Chem. Phys. 5, 2771–2785.

Palau, J.L., Pérez-Landa, G., Millán, M., 2009. Transitional dispersive scenarios driven by mesoscale flows on complex terrain under strong dry convective conditions. Atmos. Chem. Phys. 9, 119–131.

Pay, M.T., Jiménez-Guerrero, P., Baldasano, J.M., 2011. Implementation of resuspension from paved roads for the improvement of CALIOPE air quality system in Spain. Atmos. Environ. 45, 802–807. http://dx.doi.org/10.1016/j.atmosenv.2010.10.032.

Pay, M.T., Jiménez-Guerrero, P., Jorba, O., Basart, S., Pandolfi, M., Querol, X., Baldasano, J.M., 2012. Spatio-temporal variability of levels and speciation of particulate matter across Spain in the CALIOPE modeling system. Atmos. Environ. 46, 376–396. http://dx.doi.org/10.1016/j.atmosenv.2011.09.049.

Pay, M.T., Baldasano, J.M., 2012. Evaluación del sistema de pronóstico de calidad del aire CALIOPE en España para el año 2011 67 pp. Available at: http://www.bsc.es/projects/earthscience/visor/bases_datos/image_viewer/docs/20120622_Informe_Evaluacion_CALIOPE_IP_2011.pdf.

Pay, M.T., Martínez, F., Guevara, M., Baldasano, J.M., 2014. Air quality at kilometre scale grid over Spanish complex terrains. Geosci. Model Dev. 7, 1979–1999. http://dx.doi.org/10.5194/gmd-7-1979-2014.

Pérez, C., Nickovic, S., Baldasano, J.M., Sicard, M., Rocadenbosch, F., Cachorro, V.E., 2006a. A long Saharan dust event over the western Mediterranean: Lidar, Sun photometer observations, and regional dust modeling. J. Geophys. Res. 111, D15214. http://dx.doi.org/10.1029/2005JD006579.

Pérez, C., Nickovic, S., Pejanovic, G., Baldasano, J.M., Ozsoy, E., 2006b. Interactive dust-radiation modeling: a step to improve weather forecasts. J. Geophys. Res. 111, D16206. http://dx.doi.org/10.1029/2005JD006717.

Philipp, A., Beck, C., Huth, R., Jacobeit, J., 2014. Development and comparison of circulation type classifications using the COST 733 dataset and software. Int. J. Climatol. http://dx.doi.org/10.1002/joc.3920.

Pleim, J.E., 2007. A combined local and nonlocal closure model for the atmospheric boundary layer. Part II: application and evaluation in a mesoscale meteorological model. J. Appl. Meteorol. Climatol. 46, 1396–1408. http://dx.doi.org/10.1175/JAM2534.1.

Puig, R., Àvila, A., Soler, A., 2008. Sulphur isotopes as tracers of the influence of a coal-fired power plant on a Scots pine forest in Catalonia (NE Spain). Atmos. Environ. 42, 733–745. http://dx.doi.org/10.1016/j.atmosenv.2007.09.059.

Putero, D., Cristofanelli, P., Laj, P., Marinoni, A., Villani, P., Broquet, A., Alborghetti, M., Bonafè, U., Calzolari, F., Duchi, R., Landi, T.C., Verza, G.P., Vuillermoz, E., Bonasoni, P., 2014. New atmospheric composition observations in the Karakorum region: influence of local emissions and large-scale circulation during a summer field campaign. Atmos. Environ. 97, 75–82. http://dx.doi.org/10.1016/j.atmosenv.2014.07.063.

Querol, X., Alastuey, A., Pandolfi, M., Reche, C., Pérez, N., Minguillón, M.C., Moreno, T., Viana, M., Escudero, M., Orio, A., Pallarés, M., Reina, F., 2014. 2001–2012 trends on air quality in Spain. Sci. Total Environ. 490, 957–969. http://dx.doi.org/10.1016/j.scitotenv.2014.05.074.

Red Eléctrica de España (REE), 2013. Informe del Sistema Eléctrico Español. Año 2012 140 pp. Available at: http://ree.es/sites/default/files/downloadable/inf_sis_elec_ree_2012_v2.pdf.

Salvador, R., Artíñano, B., Millán, M., 1992. Aplicación de un modelo de dispersión de contaminantes para fuente puntual durante condiciones de brisa marina. Energía 2, 133–138.

Segura, S., Estellés, V., Esteve, A.R., Utrillas, M.P., Martínez-Lozano, J.A., 2013. Analysis of a severe pollution episode in Valencia (Spain) and its effect on ground level particulate matter. J. Aerosol Sci. 56, 41–52. http://dx.doi.org/10.1016/j.jaerosci.2012.06.007.

Shahgedanova, M., Burt, T.P., Davies, T.D., 1998. Synoptic climatology of air pollution in Moscow. Theor. Appl. Climatol. 61, 85–102. http://dx.doi.org/10.1007/s007040050054.

Skamarock, W.C., Klemp, J.B., 2008. A time-split nonhydrostatic atmospheric model for weather research and forecasting applications. J. Comput. Phys. 227, 3465–3485. http://dx.doi.org/10.1016/j.jcp.2007.01.037.

Tang, M.J., Cox, R.A., Kalberer, M., 2014. Compilation and evaluation of gas phase diffusion coefficients of reactive trace gases in the atmosphere: volume 1. Inorganic compounds. Atmos. Chem. Phys. 14, 9233–9247. http://dx.doi.org/10.5194/acp-14-9233-2014.

Thunis, P., Cuvelier, C., 2014. DELTA Version 4.0. Joint Research Center, Ispra (http://aqm.jrc.ec.europa.eu/DELTA/assessment/data/DELTA_UserGuide_V4_0.pdf).

Valverde, V., Pay, M.T., Baldasano, J.M., 2014. Circulation-type classification derived on a climatic basis to study air quality dynamics over the Iberian Peninsula. Int. J. Climatol. http://dx.doi.org/10.1002/joc.4179.

Vivanco, M.G., Palomino, I., Garrido, J.L., González, M.A., Alonso, G., Martín, F., 2012. Impact of the transboundary transport of air pollutants on air quality in Spain. J. Environ. Prot. 3, 1167–1175. http://dx.doi.org/10.4236/jep.2012.329135.

World Health Organization (WHO), 2013. Review of Evidence on Health Aspects of Air Pollution — REVIHAAP Project: Final Technical Report 309 pp. Available at: http://www.euro.who.int/__data/assets/pdf_file/0004/193108/REVIHAAP-Final-technical-report-final-version.pdf?ua=1.

Please cite this article as: Valverde, V., et al., A model-based analysis of SO_2 and NO_2 dynamics from coal-fired power plants under representative synoptic circulation types over the Iberian Peninsula..., Sci Total Environ (2015), http://dx.doi.org/10.1016/j.scitotenv.2015.09.111